Supporting information for:

Remote stereocentres do not disrupt the stereochemical coupling in homochiral $[M_2L_3]$ helicates and $[M_4L_6]$ tetrahedra

Rashid G. Siddique,[a] Jacob J. Whittaker, [a] Hydar A. AL-Fayaad, [a] John C. McMurtrie[b] and Jack K. Clegg[a]*

[a] School of Chemistry and Molecular Biosciences, The University of Queensland, St. Lucia, Queensland, 4072, Australia. j.clegg@uq.edu.au

[b] School of Chemistry and Physics and Centre for Materials Science, Queensland University of Technology (QUT), Brisbane, Queensland 4000, Australia

Experimental

General

All reagents were purchased from commercial sources and used without further purification. Solvents were dried using Innovative Technologies Pure Solv solvent purification system. NMR spectra were recorded on Bruker Avance 300 MHz, Bruker ASCEND 500MHz spectrometer. All DOSY experiments were performed on Bruker AVANCE 500 MHz spectrometer using standard Bruker program, ledbpg2s. A stimulated echo and longitudinal eddy-current delay (LED) was employed using bipolar gradient pulses for diffusion. In a typical DOSY experiment, the gradient pulse duration was varied between 2 and 2.4 ms, the diffusion time was 20 ms, a series of 16 spectra on 32K data points were recorded and the pulse gradients were incremented from 5 to 95%. The data was processed using Bruker Topspin 3.6 and MestReNova v. 12 and the Stokes-Einstein equation was employed to calculate the hydrodynamic radius from the resulting diffusion coefficient. Mass spectrometry was performed on Bruker MicroTOFQ, Bruker HCT and Thermo LCQ Fleet mass spectrometers using stated solvent. The University of Queensland SCMB Microanalytical Service was used for elemental microanalysis. Specific optical rotation measurements were performed on JASCO P-2000 Polarimeter at room temperature.

Synthesis

Methyl (S)-2-azidopropanoate

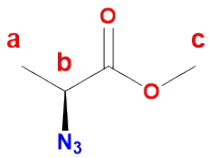

Sodium azide (6 g, 92.29 mmol) was stirred in water (8 mL) and DCM (30 mL) at room temperature for 30 min. The reaction mixture was cooled at 0 °C and triflic anhydride (3 mL, 17.83 mmol) was added dropwise and stirred the mixture for 2 h at 0 °C. The organic phase was separated, and water layer was extracted with 10 mL DCM. The combined organic layers were washed with saturated solution of $NaHCO_3$, brine and then dried over $MgSO_4$. The resulting freshly prepared trifluoromethanesulfonyl azide was immediately added into the solution of *L*-alanine methyl ester hydrochloride (0.8 g, 5.73 mmol), $CuSO_4 \cdot 5H_2O$ (30 mg, 0.12 mmol) in DCM (10 mL). The slurry was stirred for 12 hours, diluted with water and extracted into DCM. The DCM layer was then passed through a silica plug and the evaporation of the filtrates resulted into pure oily product (0.74 g, 60%).

^{1}H NMR (300 MHz, $CDCl_3$, δ/ppm): 1.49 (d, 3H^{a}), 3.96 (q, 1H^{b}), 3.80 (s, 3H^{c}). The ^{1}H NMR was matched with previously reported procedure[1].

CAUTION: Trifluoromethanesulfonyl azide should be prepared in dilute DCM because it may lead to an explosion in the absence of solvent[2].

Synthesis of dimethyl 2,2'-((2,5-di([2,2'-bipyridin]-5-yl)-1,4-phenylene)bis(1H-1,2,3-triazole-4,1-diyl)) dipropionate (L^3)

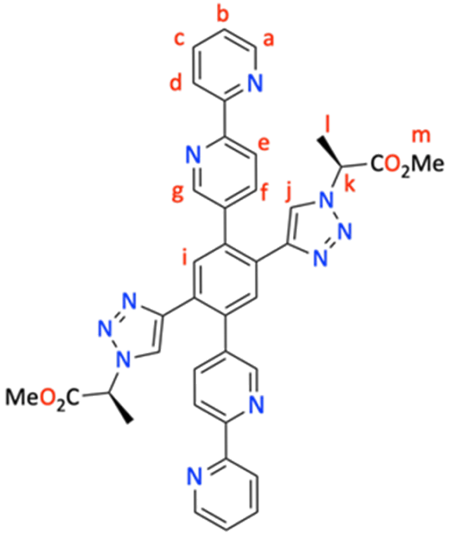

L^3

The ligand L^3 was synthesized by reacting L^1 (0.15 g, 0.345 mmol) with *L*-alanine azide (0.19 g, 1.408 mmol) using $[Cu(CH_3CN)_4PF_6]$ (39 mg, 0.104 mmol) at 70°C for 2d under N_2 atmosphere. The reaction mixture was concentrated under reduced pressure and diluted with 100 mL chloroform and 100 mL saturated Na_2-EDTA solution. The resulting mixture was stirred for 3h, separated organic layer and the aqueous layer was extracted two times with chloroform. The combined organic layers were washed with Na_2-EDTA solution, brine and dried over $MgSO_4$. The resulting product after removal of solvent was washed with minimum amount of cold methanol and the off-white precipitates were collected. 2D COSY and 1D NOESY proton NMR were carried out to assign peaks. ^{1}H NMR (500 MHz, $CDCl_3$, δ/ppm, J/Hz): 1.72-1.67 (d, $6H^l$, 7.4 Hz), 3.69 (s, $6H^m$), 5.31-5.38 (q, $2H^k$, 7.4 Hz), 6.98 (s, $2H^j$), 7.35-7.41 (m, $2H^b$), 7.85-7.93 (m, $2H^e$ and $2H^f$), 8.20 (s, $2H^i$), 8.45-8.50 (d, $2H^c$, 8.3 Hz), 8.50-8.55 (d, $2H^d$, 8.2 Hz), 8.72-8.68 (m, $2H^a$), 8.73-8.76 (m, $2H^g$), Positive ion ESI-HRMS: *m/z* (M=$C_{38}H_{32}N_{10}O_4$; in DCM/Methanol): calcd for $[M+H]^+$ 693.26, found 693.26, cald for $[M+Na]^+$ 715.25, found 715.25. Elemental Analysis (%) calcd: C, 65.89; H, 4.66; N, 20.22; Found: C, 65.62; H, 4.58, N, 19.92. Specific optical rotation [αD] at 22° C in chloroform = 30.63.

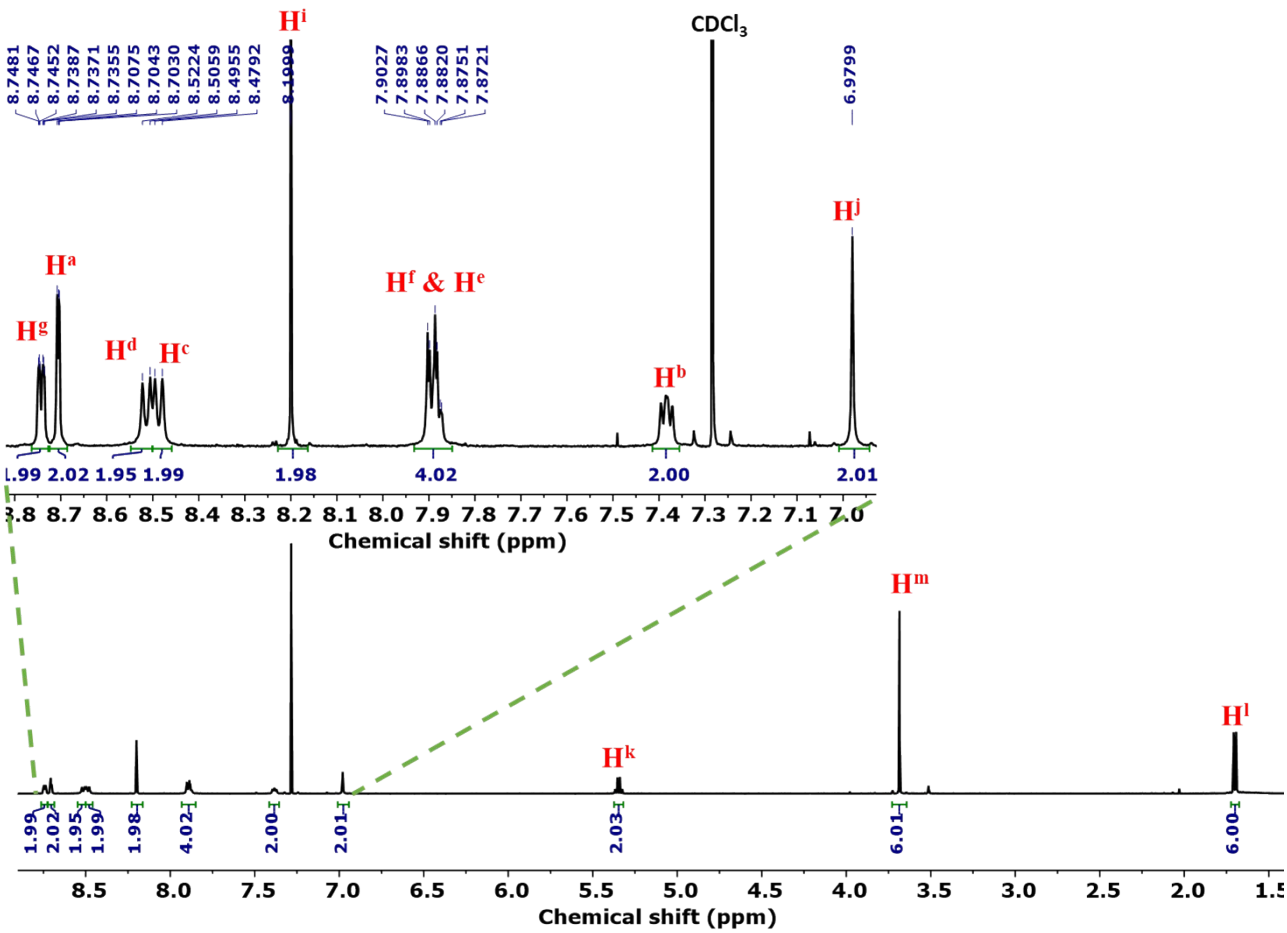

Figure S1: ^{1}H NMR spectrum (500 MHz, $CDCl_3$, 298K) of ligand **L^3** with peak assignments.

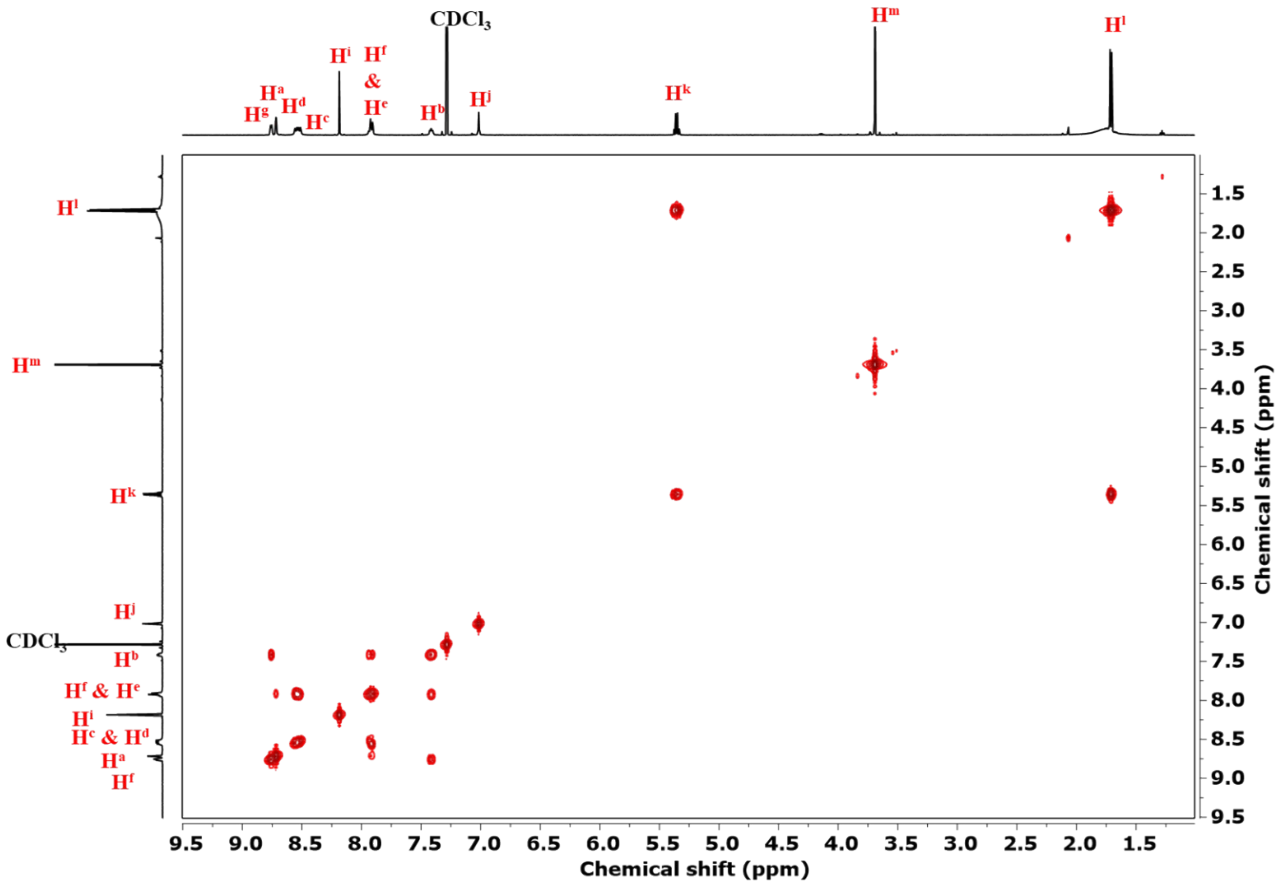

Figure S2: ^{1}H-^{1}H COSY spectrum ($CDCl_3$, 500 MHz, 298K) of ligand **L^{3}**.

Synthesis of methyl 2-(4-(2,5-di([2,2'-bipyridin]-5-yl)phenyl)-1H-1,2,3-triazol-1-yl) propanoate (L^4)

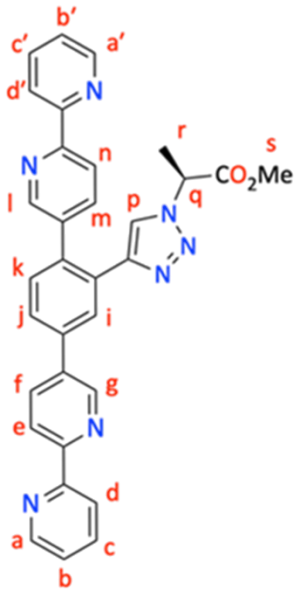

L^4

The ligand **L^4** was synthesized by reacting **L^2** (0.1g, 0.24 mmol) with *L*-alanine azide (0.095g, 0.704 mmol) in acetonitrile (15 mL) using $[Cu(CH_3CN)_4PF_6]$ (39 mg, 0.104 mmol) at 70 °C for 2d under N_2 atmosphere. The reaction mixture was concentrated under reduced pressure and diluted with chloroform (100 mL) and saturated Na_2-EDTA solution (100 mL). The resulting mixture was stirred for 3h, separated organic layer and the aqueous layer was extracted two times with chloroform. The combined organic layers were washed with Na_2-EDTA solution, brine and dried over $MgSO_4$. After removal of solvent the resulting product was washed with minimum amount of cold methanol and the off-white precipitates were collected (0.08 g, 61%). 2D COSY and a series of 1D NOESY proton NMR experiments were carried out to assign peaks.

^{1}H NMR (500 MHz, $CDCl_3$, δ/ppm): 1.70 (d, 7.4 Hz, H^r), 3.67 (s, H^s), 5.37 (q, 7.4 Hz, H^q), 7.00 (s, H^p), 7.35-7.38 (m, $2H^{bb'}$), 7.55 (d, 7.9 Hz, $1H^n$), 7.77-7.82 (m, H^f and H^m), 7.85-7.90 (m, $2H^{cc'}$), 8.18 (dd, 8.3 and 2.4 Hz, $1H^j$), 8.40 (d, 2.0 Hz, H^g), 8.45-8.48 (m, $2H^e$), 8.49-8.51 (m, H^k), 8.66 (dd, 2.4 and 0.8 Hz, H^l), 8.71-8.76 (m, $2H^{aa'}$), 9.06-9.08 (dd, 2.4 and 0.8 Hz, H^i), 8.44-8.48 (m, $2H^{dd'}$). ^{13}C NMR (500MHz, $CDCl_3$, δ/ppm): 169.29, 155.76, 155.63, 155.32, 155.11, 149.41, 149.28, 149.23, 147.46, 146.03, 138.09, 137.87, 137.07, 136.5, 136.38, 135.46, 135.48, 131.31, 130.37, 128.34, 127.1, 123.97, 123.86, 122.0, 121.26, 121.13, 120.57, 58.15, 53.11,18.01. Positive ion ESI-HRMS: *m/z* ($C_{32}H_{25}N_7O_2$; in DCM):

calcd for $[M+H]^+$ 540.21479, found 540.16. Elemental Analysis (%) calcd: C, 71.21; H, 4.67; N, 18.17; Found: C, 70.91; H, 4.60; N, 18.0. Specific optical rotation [αD] at 22° C in chloroform = 16.84.

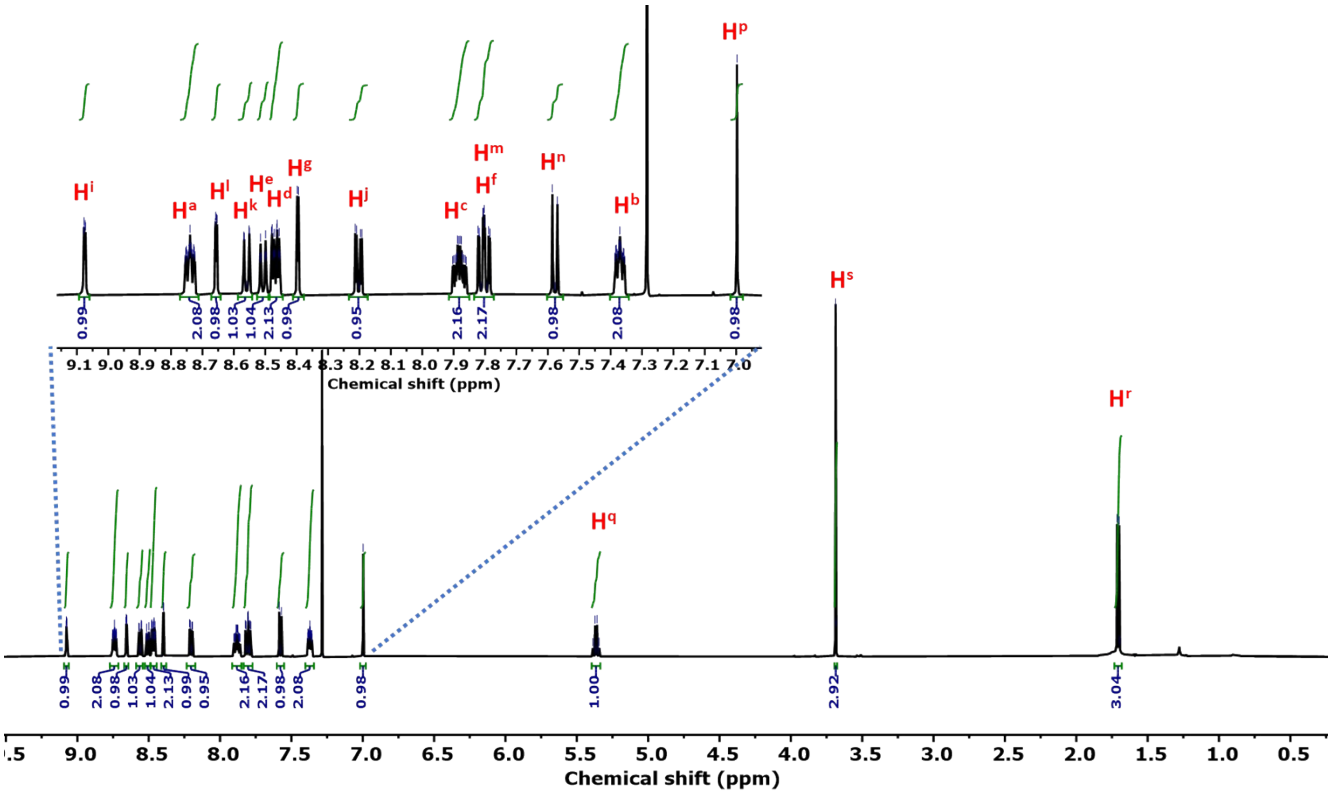

Figure S3: ^{1}H NMR spectrum (500 MHz, $CDCl_3$, 298K) of ligand **L^4** with peak assignments.

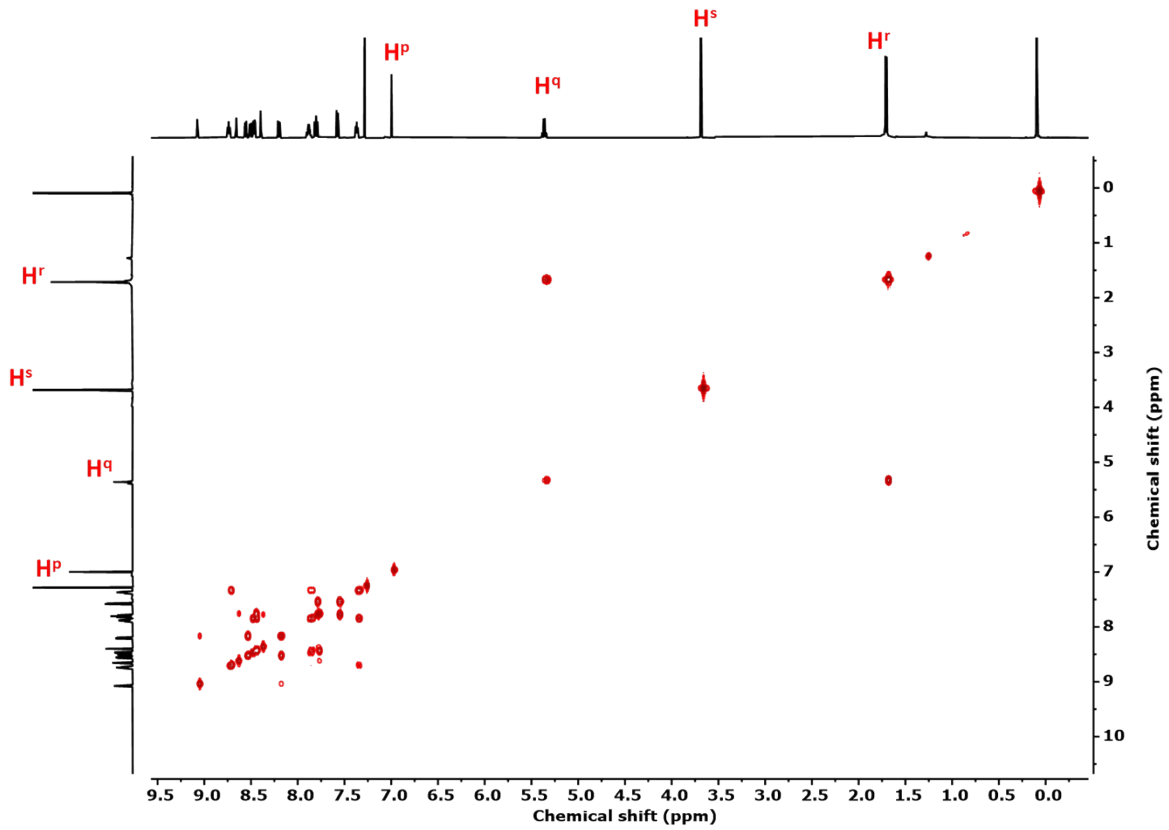

Figure S4: ^{1}H-^{1}H COSY spectrum ($CDCl_3$, 500 MHz, 298K) of ligand **L^4**.

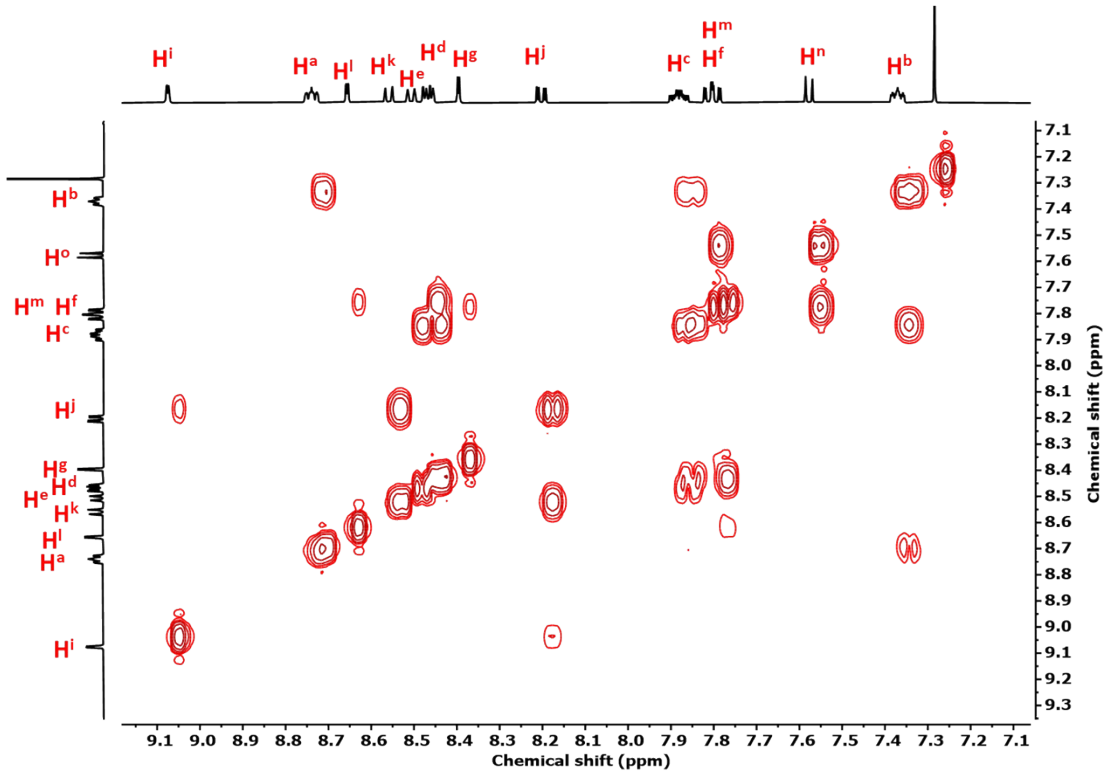

Figure S5: ^{1}H-^{1}H COSY spectrum ($CDCl_3$, 500 MHz, 298K) of ligand **L^4** in the aromatic region.

Synthesis of $[Fe_2(L^3)_3](BF_4)_4$

The $\mathbf{L^3}$ (16.6 mg, 0.024mmol) and $Fe(BF_4)_2.6H_2O$ (5.4mg, 0.016 mmol) were mixed into acetonitrile (2.5 mL) solution and the reaction mixture was heated in microwave for 30 minutes at 130°C that give quantitative amount of single assembly.

^{1}H NMR (500MHz, CD_3CN, δ/ppm) of $[Fe_2(\mathbf{L^3})_3](BF_4)_4$: 1.43 (d, H^l), 1.86 (d, H^l), 3.64 (s, H^m), 3.74 (s, H^m), 5.20 (q, H^k), 5.55 (q, H^k), 7.09 (d, H^a), 7.13 (d, H^a), 7.30 (s, H^g), 7.34 (s, H^g), 7.47-7.54 (m, H^b), 7.81 (s H^j), 7.86 (s, H^j), 7.88 (s, H^i), 7.99 (s, H^i), 8.12-8.26 (m, H^c and H^f), 8.45 (d, H^d), 8.49 (d, H^d), 8.59 (d, H^e) 8.65 (d, H^e). ^{1}H DOSY NMR: 11.4Å hydrodynamic radius. Positive ion ESI-HRMS: m/z (M= $[Fe_2(C_{38}H_{32}N_{10}O_4)_3](BF_4)_4$ in acetonitrile); calculated $(M\text{-}2BF_4)^{2+}$ m/z = 1181.8373, found m/z = 1181.83; calculated $(M\text{-}3BF_4)^{3+}$ m/z = 758.8893, found m/z = 758.89; calculated $(M\text{-}4BF_4)^{4+}$ m/z = 547.4154, found m/z = 547.41.

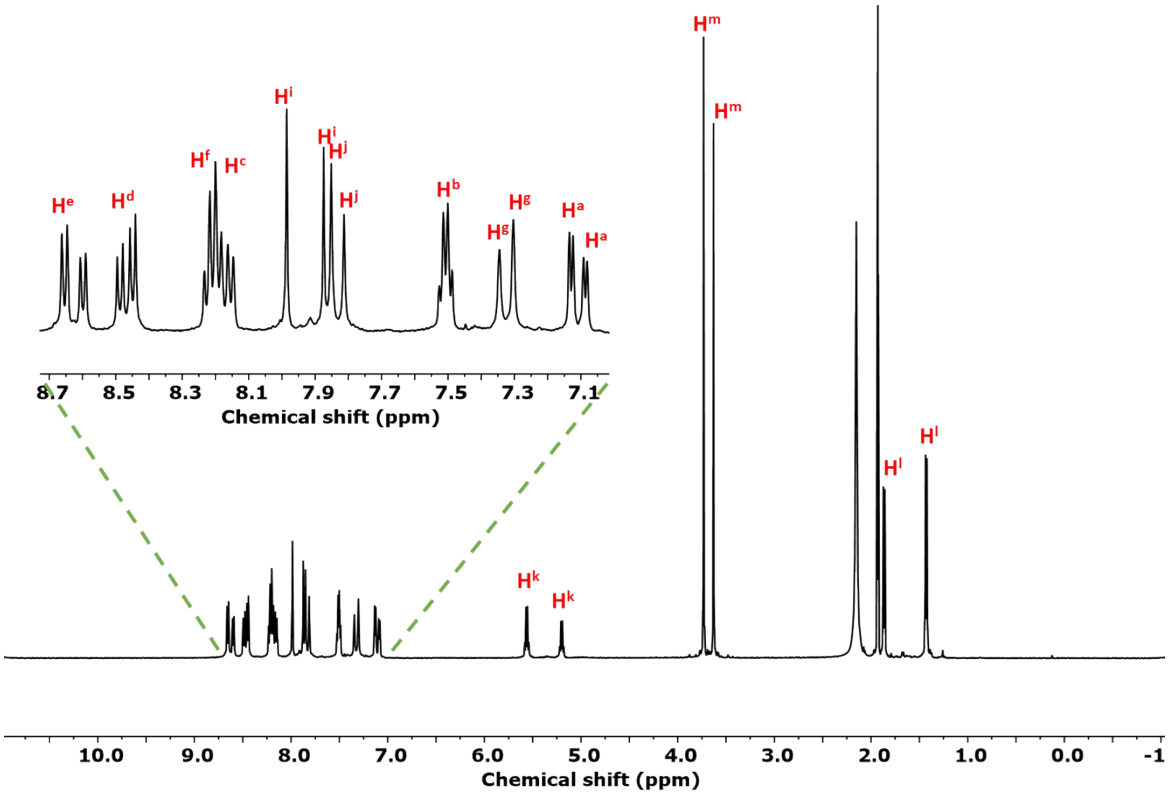

Figure S6: ^{1}H NMR spectrum (CD_3CN, 500 MHz, 298 K) of $[Fe_2\mathbf{L^3}_3](BF_4)_4$ helicate.

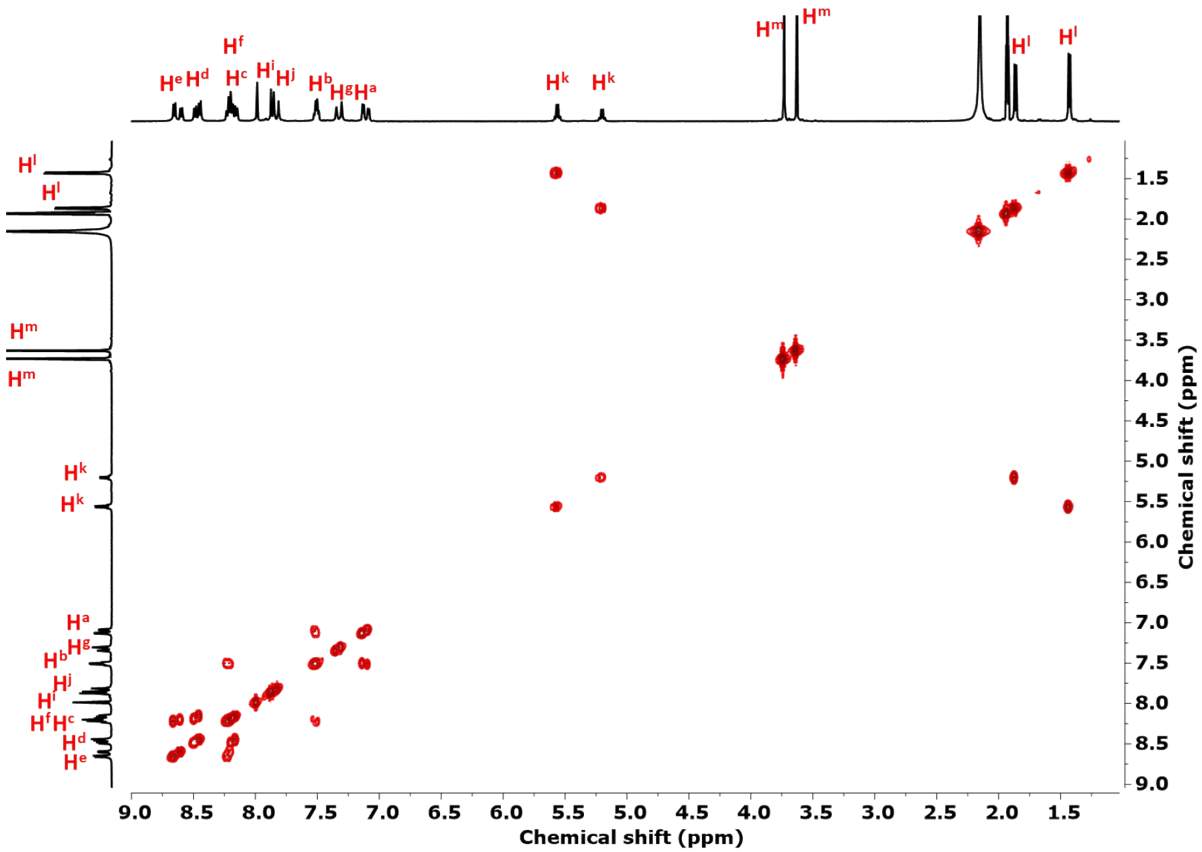

Figure S7: ^{1}H-^{1}H COSY spectrum (CD_3CN, 500 MHz, 298 K) of $[Fe_2\mathbf{L}^{3}_3](BF_4)_4$ helicate.

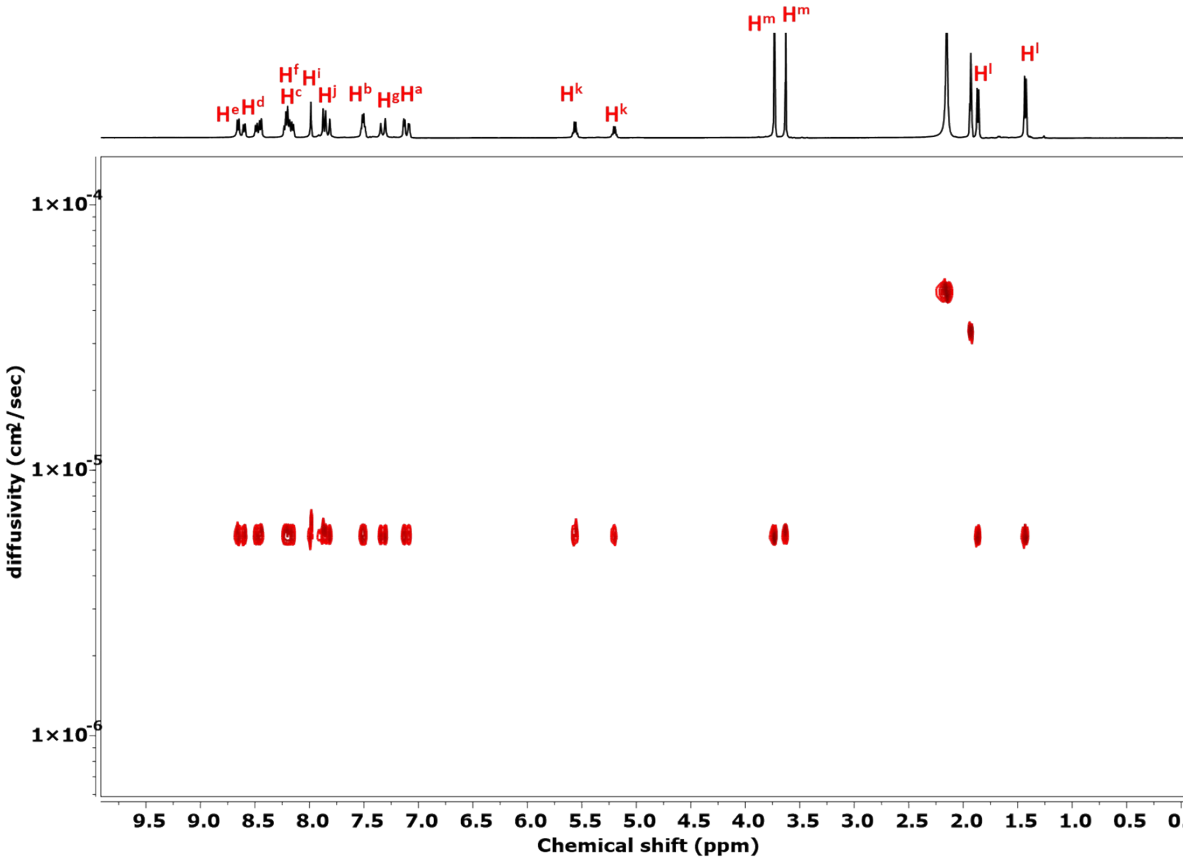

Figure S8: ^{1}H 2D DOSY NMR (500 MHz, CD_3CN, 298K) of $[Fe_2\mathbf{L}^{3}_3](BF_4)_4$ helicate.

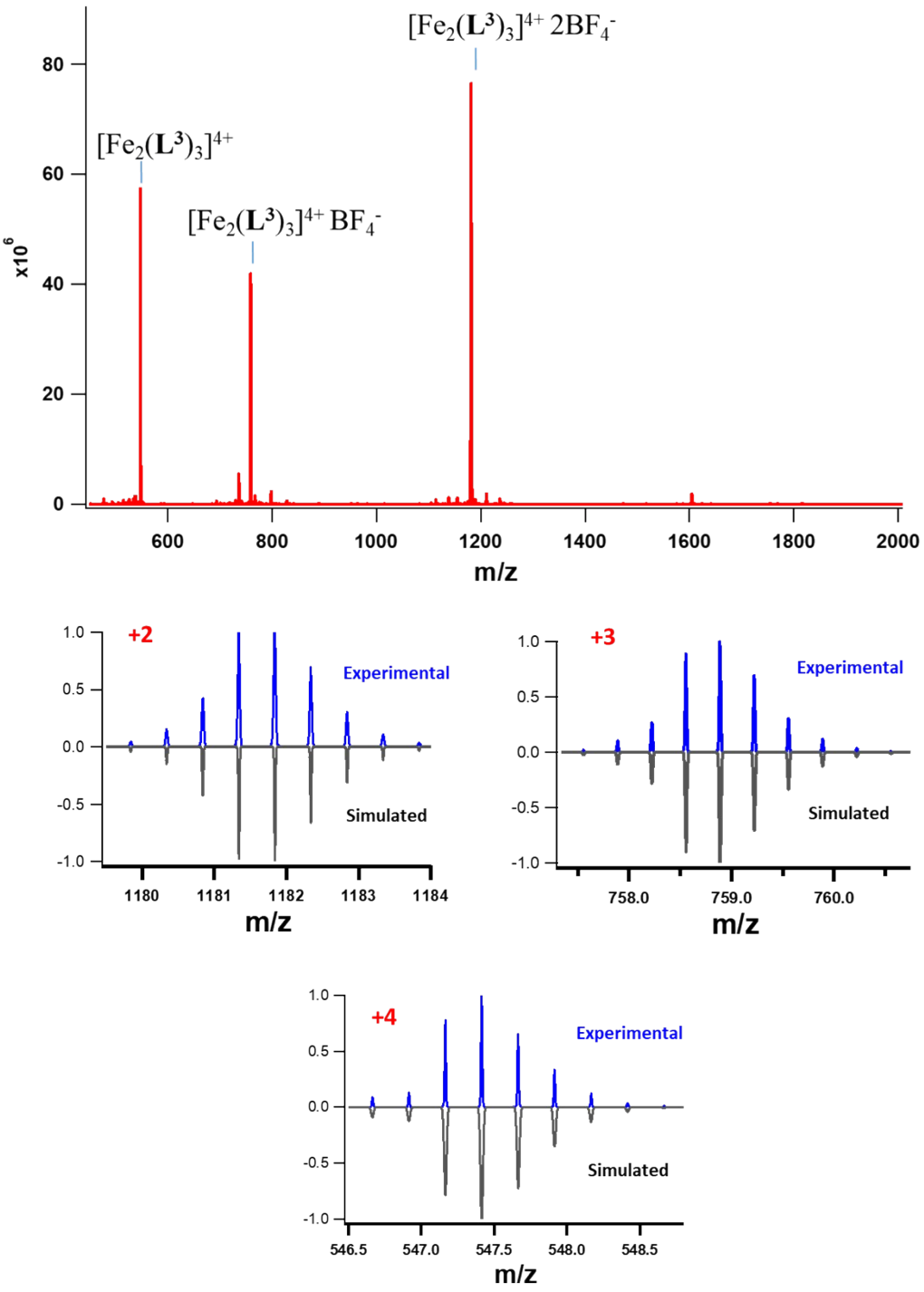

Figure S9: ESI-MS of the product +2, +3 and +4 ions detected that correspond to 2, 3 and 4 losses of BF_4^- ions from an $[Fe_2\mathbf{L^3}_3](BF_4)_4$.

Synthesis of $[Co_2(L^3)_3](ClO_4)_4$

The helical self-assembly of cobalt (II) was obtained by reacting cobalt(II) perchlorate (5.9 mg, 0.016 mmol) with ligand $\mathbf{L^3}$ (16.6 mg, 0.024mmol) in acetonitrile (2.5 mL) under similar microwave conditions as used for iron (II) complexes. The resulting orange solution contains quantitative amount of single assembly. Long range ^{1}H NMR (500MHz, CD_3CN, -60 to 230 ppm) of $[Co_2(\mathbf{L^3})_3](ClO_4)_4$: 158.16, 151.80, 148.89, 143.47, 72.40, 71.43, 71.05, 70.36, 51.80, 50.07, 9.86, 9.61, 9.40, 8.08, 7.27, 7.12, 5.54, 5.02, 3.62, 3.41, 1.79, 1.63, 1.27, 1.21. Positive ion ESI-HRMS: m/z (M= $[Co_2(C_{38}H_{32}N_{10}O_4)_3](ClO_4)_4$ in acetonitrile); calculated $(M\text{-}2ClO_4)^{2+}$ m/z = 1197.2728, found m/z = 1197.28; calculated $(M\text{-}3ClO_4)^{3+}$ m/z = 764.8657, found m/z = 764.87; calculated $(M\text{-}4ClO_4)^{4+}$ m/z = 548.9121, found m/z = 548.91.

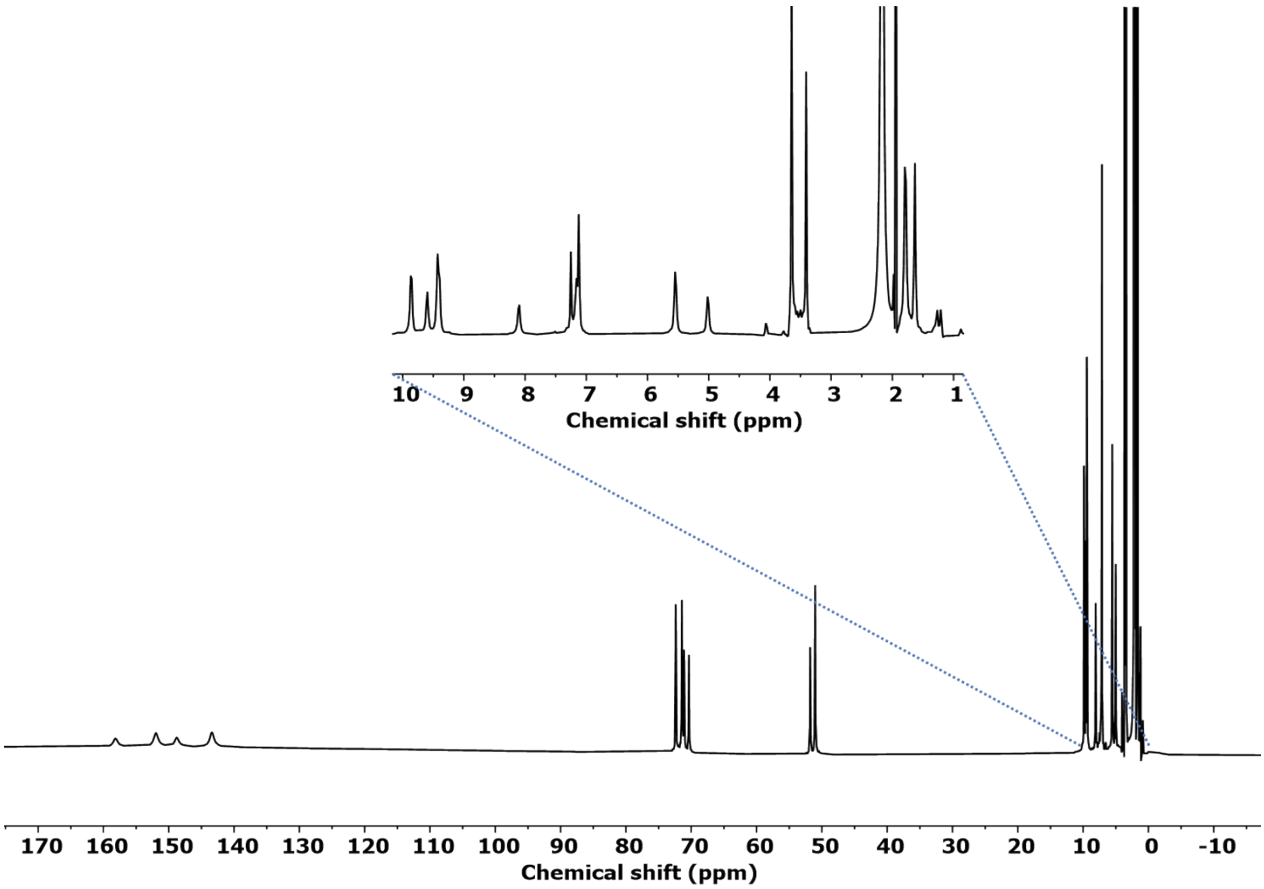

Figure S10: ^{1}H NMR spectrum (CD_3CN, 500 MHz, 298 K) of $[Co_2\mathbf{L^3}_3](ClO_4)4$ helicate.

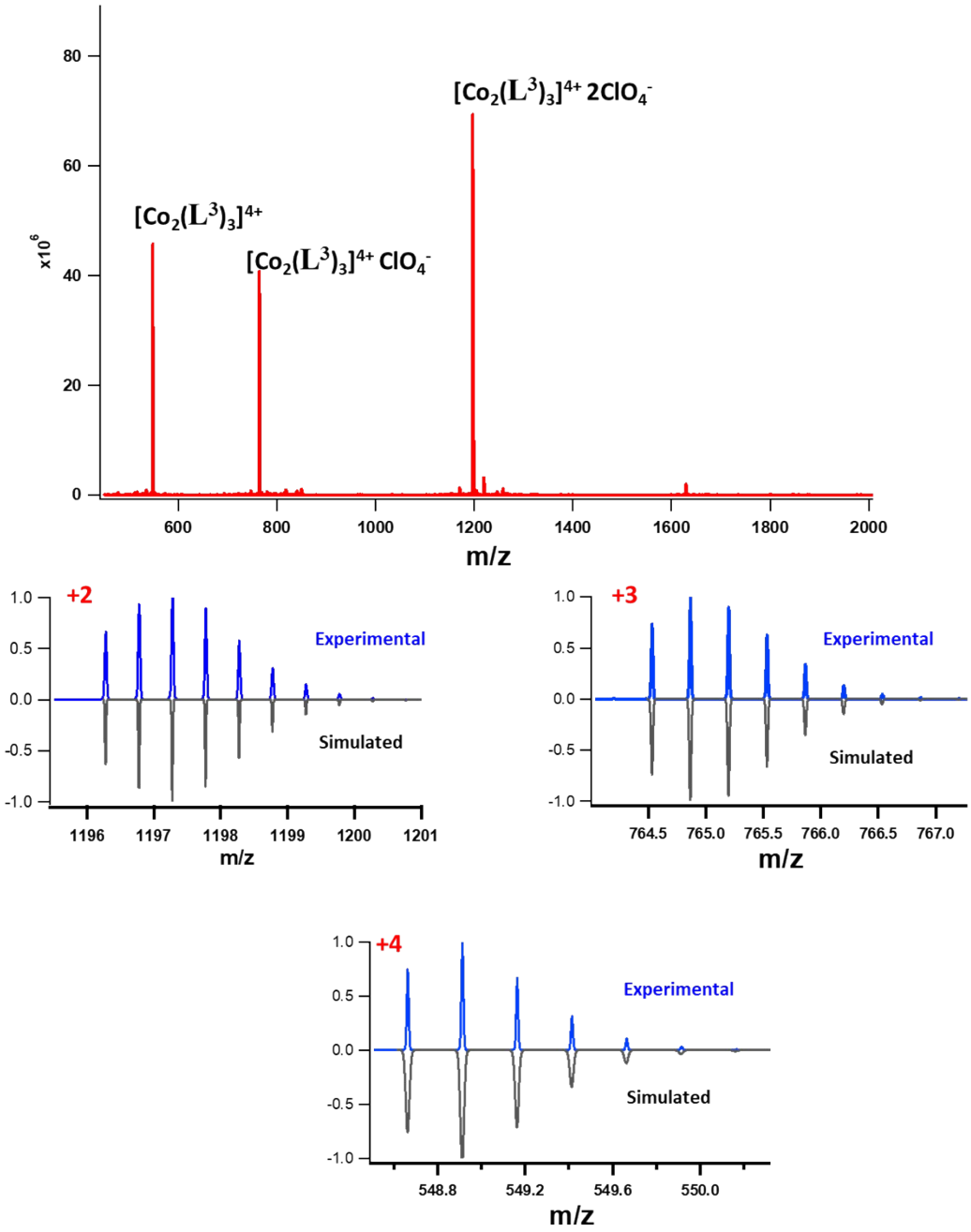

Figure S11: ESI-MS of the product +2, +3 and +4 ions detected that correspond to 2, 3 and 4 losses of ClO_4^- ions from an $[Co_2\mathbf{L}^3_3](ClO_4)_4$.

Synthesis of $[Co_2(L^3)_3](PF_6)_6$

The Co(II) helical assembly was then oxidized by adding solution of ammonium cerium(IV) nitrate (13mg, 0.0237 mmol, 5mL acetonitrile) into the above $[Co_2(\mathbf{L^3})_3](ClO_4)_4$ assembly. The resulting mixture was stirred overnight, and the precipitates were collected and washed with acetonitrile. The precipitates were then re-dissolved in the 2:1 mixture of water and acetonitrile (6 ml). The addition of saturated solution of KFP_6 to the above assembly solution resulted in the formation of precipitates, which were collected and washed with water. The deep orange product was then dried under high vac that gave 22.5 mg (90%) yield.

The ^{1}H NMR (500MHz, CD_3CN, δ/ppm) of $[Co_2(\mathbf{L^3})_3](PF_6)_6$: 1.71 (d, H^l), 1.94 (d, H^l), 3.76 (s, H^m), 3.86 (s, H^m), 5.36 (q, H^k), 5.74 (q, H^k), 7.11 (d, H^a), 7.22 (d, H^a), 7.34 (s H^j), 7.37 (s, H^j), 7.69 (s, H^g), 7.79 (s, H^g), 7.81-7.85 (m, H^b), 7.87 (s, H^i), 8.16 (s, H^i), 8.37 (d, H^f), 8.49 (d, H^f), 8.54-8.62 (m, H^c) 8.68 (d, H^d), 8.73 (d, H^d), 8.78 (d, H^e) 8.86 (d, H^e). ^{1}H DOSY NMR: 12.7 Å hydrodynamic radius. Positive ion ESI-HRMS: m/z (M= $[Co_2(C_{38}H_{32}N_{10}O_4)_3](PF_6)_6$ in acetonitrile) ; calculated $(M\text{-}2PF_6)^{2+}$ m/z = 1387.75, found m/z = 1387.75; calculated $(M\text{-}3PF_6)^{3+}$ m/z = 876.84, found m/z = 876.84; calculated $(M\text{-}4PF_6)^{4+}$ m/z = 621.39, found m/z = 621.39, calculated $(M\text{-}5PF_6)^{5+}$ m/z = 468.12, found m/z = 468.12, calculated $(M\text{-}6PF_6)^{6+}$ m/z = 365.94, found m/z = 365.94.

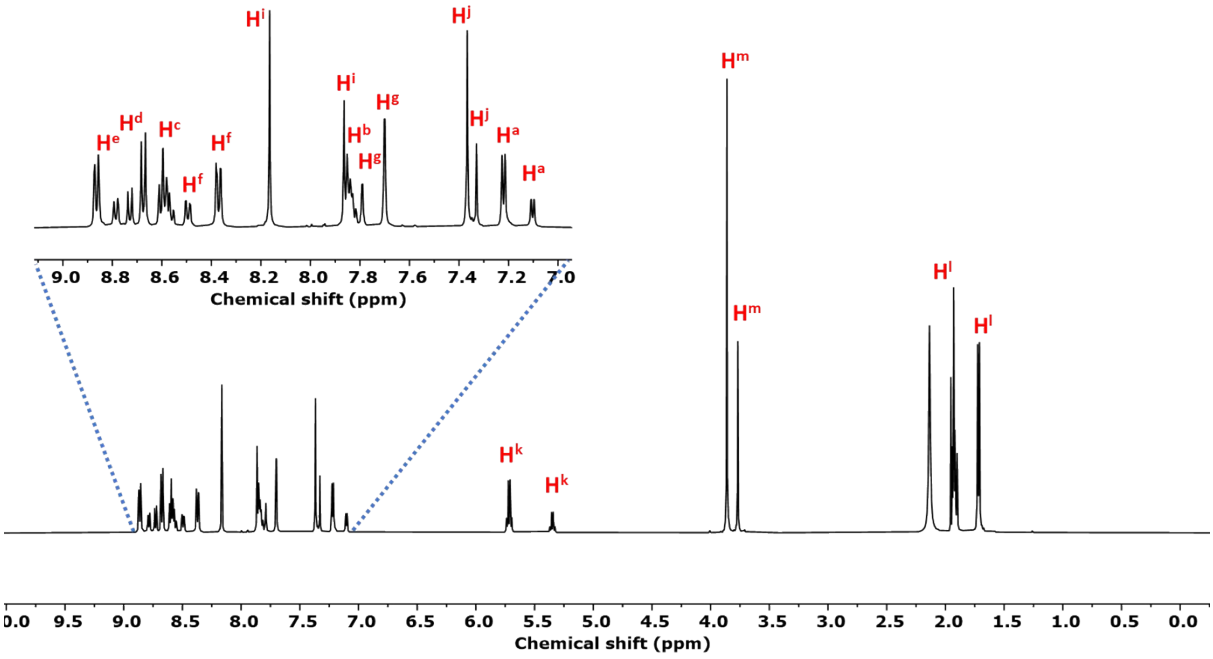

Figure S12: ^{1}H NMR spectrum (CD_3CN, 500 MHz, 298 K) of $[Co_2\mathbf{L^3}_3](PF_6)_6$ helicate.

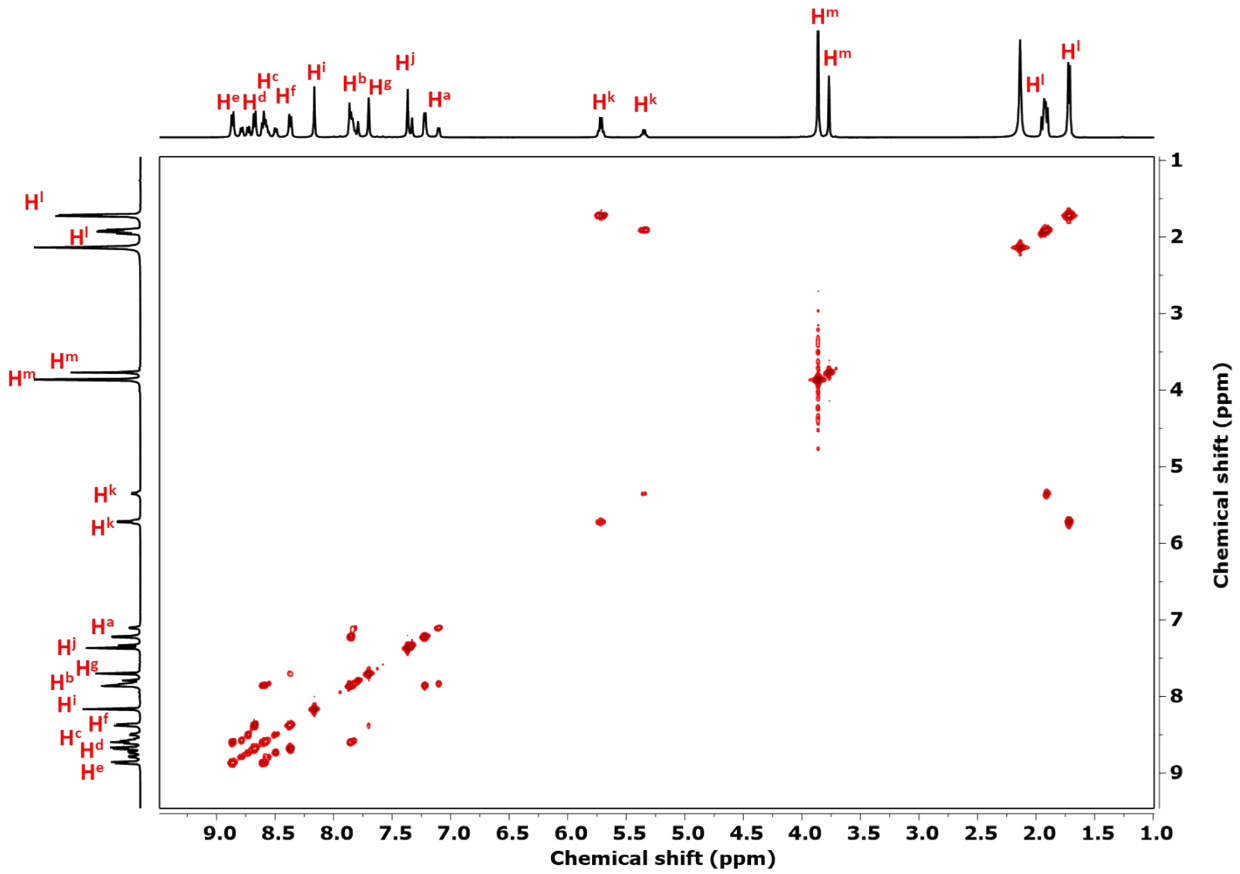

Figure S13: ^{1}H-^{1}H COSY spectrum (CD_3CN, 500 MHz, 298 K) of $[Co_2\mathbf{L}^{3}_3](PF_6)_6$ helicate.

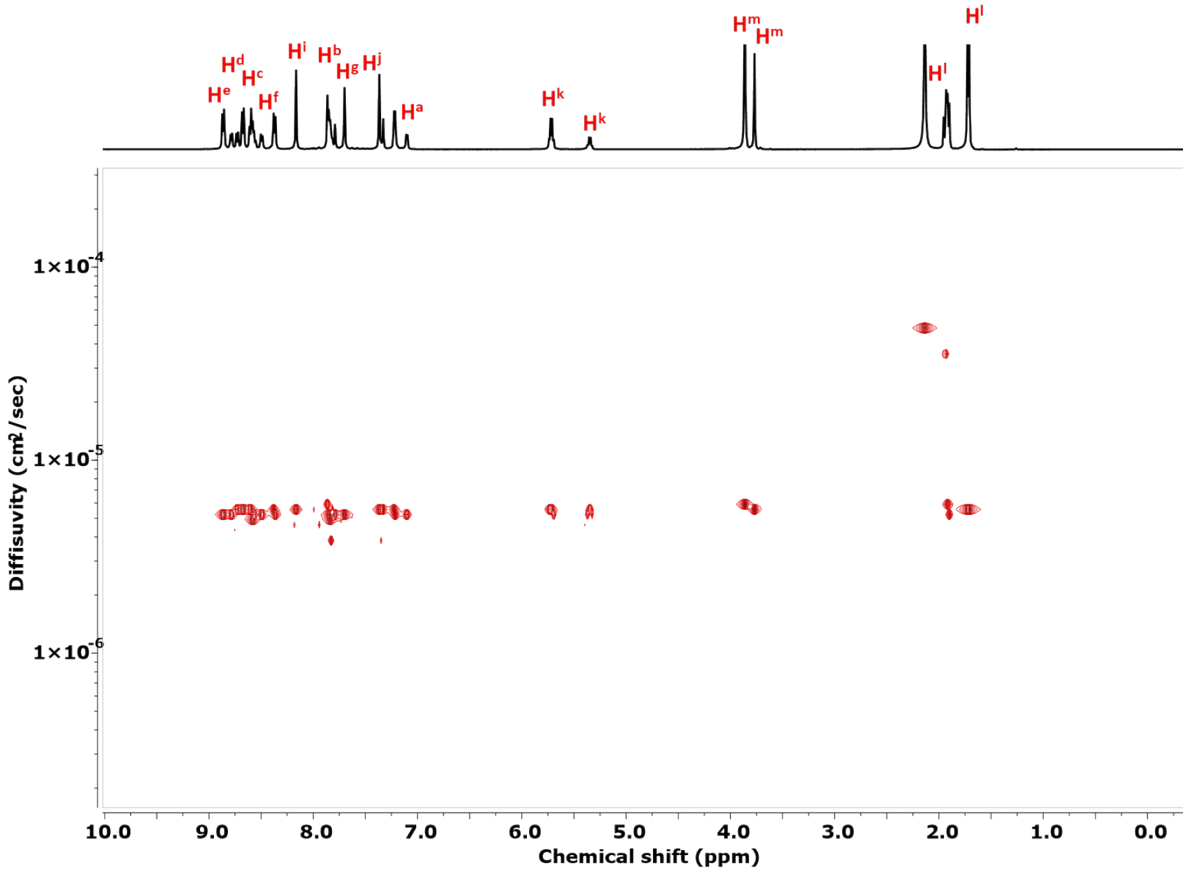

Figure S14: ^{1}H 2D DOSY NMR (500 MHz, CD_3CN, 298K) of $[Co_2\mathbf{L}^{\mathbf{3}}_3](PF_6)_6$ helicate.

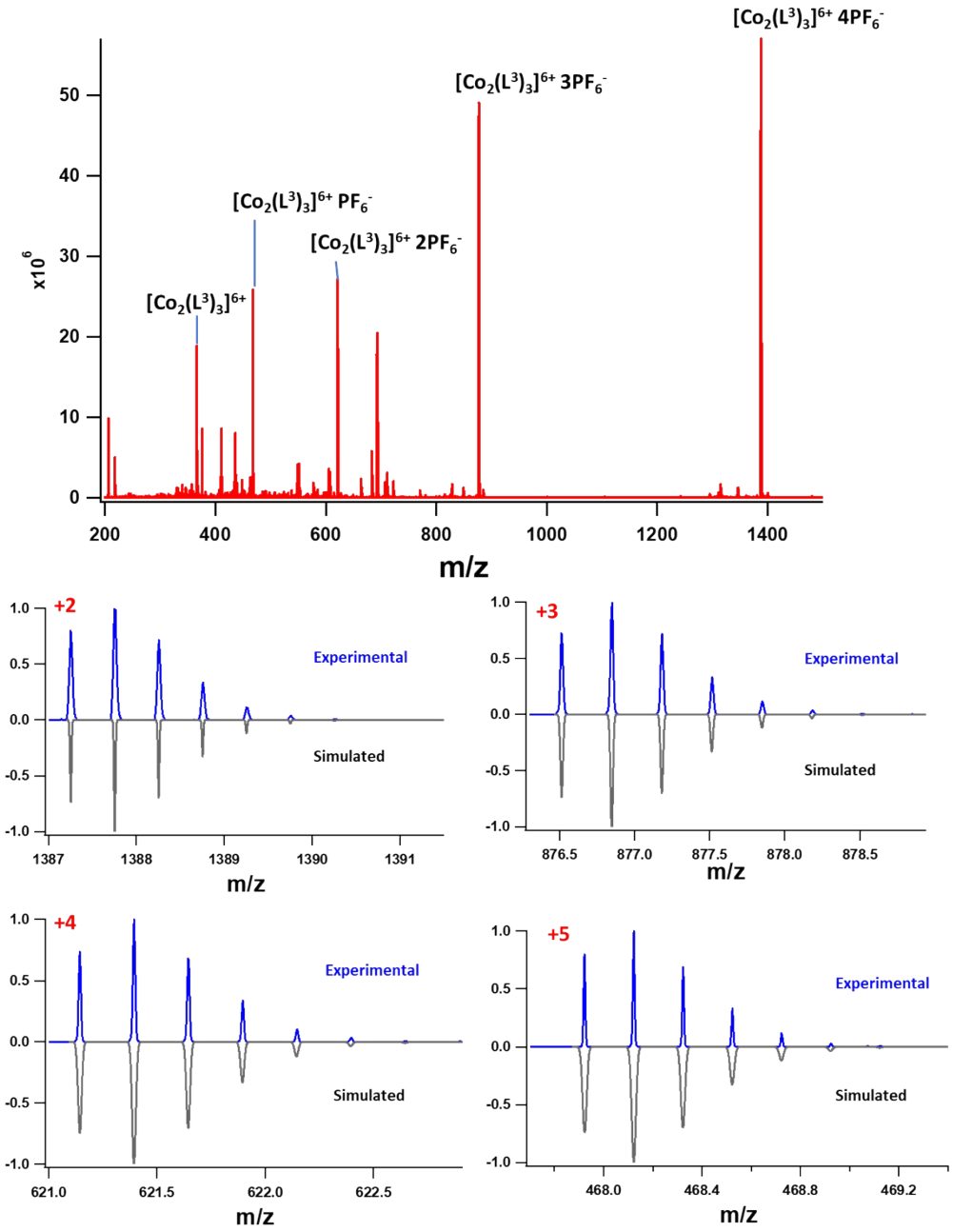

Figure S15: ESI-MS of the product +2, +3, +4, +5 and +6 ions detected that correspond to 2, 3, 4, 5 and 6 losses of PF_6^- ions from an $[Co_2\mathbf{L}^3_3](PF_6)_6$.

Synthesis of $[Fe_2(L^4)_3](PF_6)_4$ and $[Fe_4(L^4)_6](PF_6)_8$

The ligand $\mathbf{L^4}$ (38 mg, 0.07 mmol) and $Fe(BF_4)_2.6H_2O$ (17.4 mg, 0.046 mmol) were mixed into acetonitrile (5 mL) and the reaction mixture was heated in microwave for 20 minutes at 130°C. The resulting solution was subjected to silica gel using acetonitrile, water and saturated KNO_3 (7:1:0.5) as eluent, followed by the addition of excess aqueous solution of KPF_6 yielded two red products. Total yield of both products was 47 mg (87%), out of which 20 mg (42%) was the lower *Rf* product and 27 mg (62%) of higher *Rf* product.

The ^{1}H NMR (500MHz, CD_3CN, δ/ppm) of first red band i.e., $[Fe_2(\mathbf{L^4})_3](PF_6)_4$: 5.47-5.10 (eight quartets of H^q for C_3 and $C_{1,}$ & C_3' and C_1' species), 3.56-3.74 (eight singlets of H^s for C_3 and $C_{1,}$ & C_3' and C_1' species), 1.25-1.83 (eight doublets of H^r for C_3 and $C_{1,}$ & C_3' and C_1' species), 6.49-7.1 (region of singlets for H^g and H^l), 7.20-7.34 (multiplets for H^a), 7.46-7.55 (multiplets for H^b), 7.51-7.76 (eight singlets of H^p for C_3 and $C_{1,}$ & C_3' and C_1' species), 8.48-8.60 (multiplets for H^d),. The ^{1}H 2D DOSY NMR (500MHz, CD_3CN, δ/ppm) of $[Fe_2(\mathbf{L^4})_3](PF_6)_4$: Recorded Diff Con. for assigned peaks $5.88e^{-10}$ m^2s^{-1}; Calculated hydrodynamic radius 11.1Å.

Positive ion ESI-HRMS: m/z (M= $[Fe_2(\mathbf{L^4})_3](PF_6)_4$ in acetonitrile); calculated $(M\text{-}2PF_6)^{2+}$ m/z = 1010.21, found m/z = 1010.21; calculated $(M\text{-}3PF_6)^{3+}$ m/z = 625.15, found m/z = 625.15; calculated $(M\text{-}4PF_6)^{4+}$ m/z = 432.62, found m/z = 432.62.

^{1}H NMR (500MHz, CD_3CN, δ/ppm) of second red band i.e., $[Fe_4(\mathbf{L^4})_6](PF_6)_8$ (**Figure S22**): 5.49-5.6 (multiplets and broader signal for H^q), 3.30-3.90 (singlets and broader signal for H^s), 1.2-2.0 (multiplets and broader signal for H^r). The aromatic region was complex and could not be assigned. The ^{1}H 2D DOSY NMR (500MHz, CD_3CN, δ/ppm) of $[Fe_4(\mathbf{L^4})_6](PF_6)_8$: Recorded diff con. for assigned peaks $4.25e^{-10}$ m^2s^{-1};Calculated hydrodynamic radius 15.4Å. ^{19}F NMR (500MHz, CD_3CN, δ/ppm) of $[Fe_4(\mathbf{L^4})_6](PF_6)_8$: -72.78.

Positive ion ESI-HRMS: m/z (M= $[Fe_4(\mathbf{L^4})_6](PF_6)_8$ in acetonitrile); calculated $(M\text{-}3PF_6)^{3+}$ m/z = 1395.27, found m/z = 1395.27; calculated $(M\text{-}4PF_6)^{4+}$ m/z = 1010.21, found m/z = 1010.21; calculated $(M\text{-}5PF_6)^{5+}$ m/z = 779.17, found m/z = 779.17, calculated $(M\text{-}6PF_6)^{6+}$ m/z = 625.15, found m/z = 625.15; calculated $(M\text{-}7PF_6)^{7+}$ m/z = 515.13, found m/z = 515.13; calculated $(M\text{-}8PF_6)^{8+}$ m/z = 432.62, found m/z = 432.62.

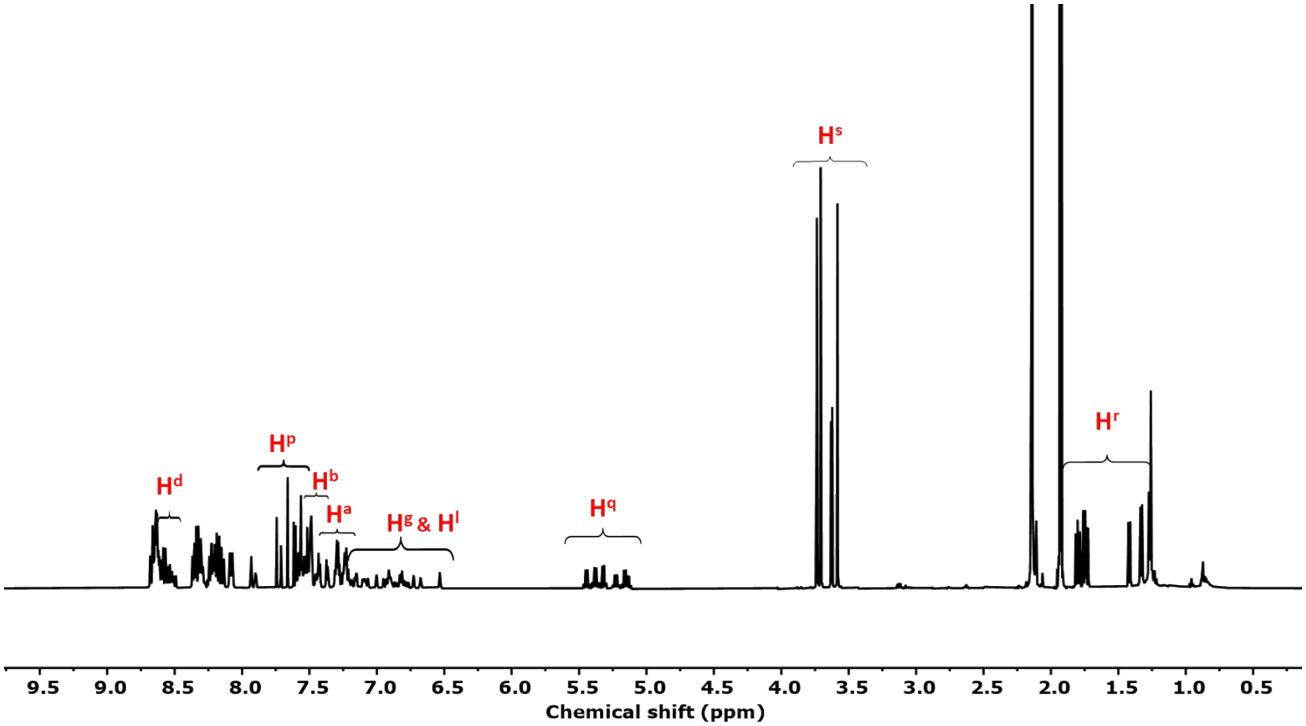

Figure S16: ^{1}H NMR spectrum (CD_3CN, 500 MHz, 298 K) of $[Fe_2\mathbf{L}^{\mathbf{4}}{}_3](PF_6)_4$ helicate.

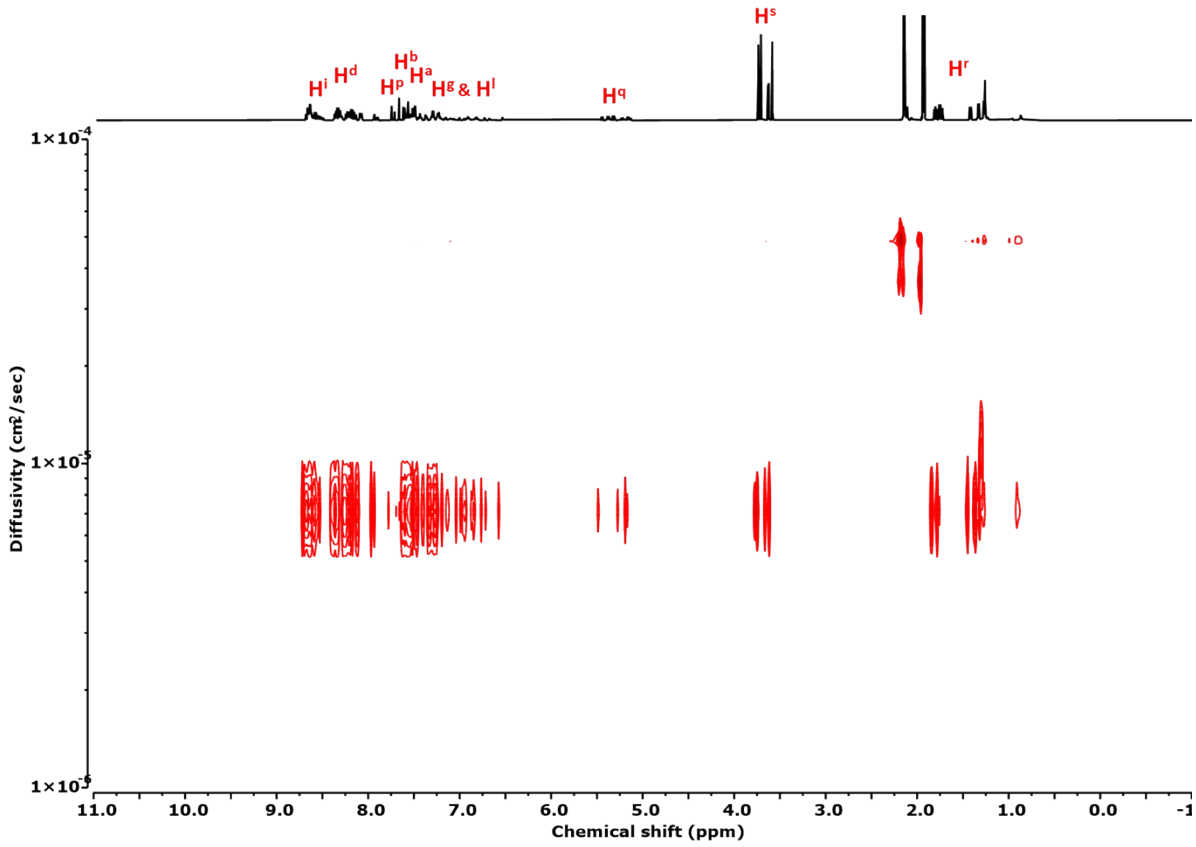

Figure S17: ^{1}H 2D DOSY NMR (500 MHz, CD_3CN, 298K) of $[Fe_2\mathbf{L}^{\mathbf{4}}{}_3]^{4+}$ helicate.

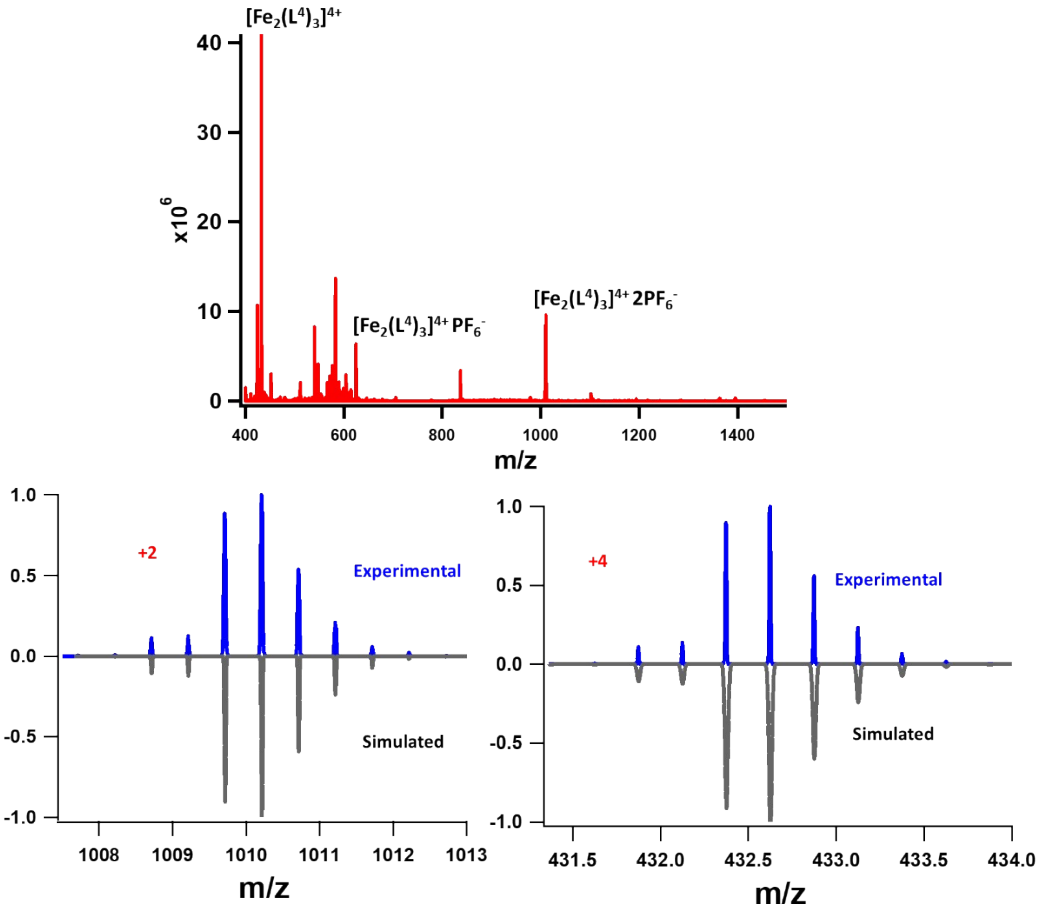

Figure S18: ESI-MS of the product +2, +3 and +4 ions detected that correspond to 2, 3 and 4 losses of PF_6^- ions from an $[Fe_2\mathbf{L}^4{}_3](PF_6)_4$.

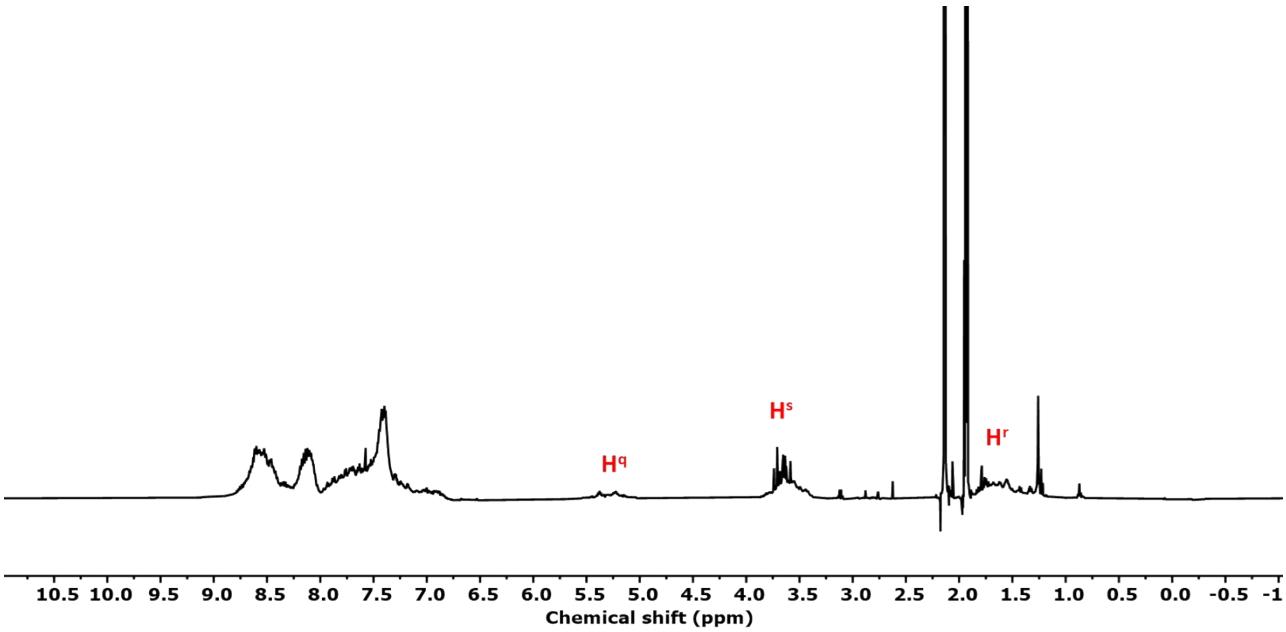

Figure S19: ^{1}H NMR spectrum (CD_3CN, 500 MHz, 298 K) of $[Fe_4\mathbf{L}^{4}_6](PF_6)_8$ tetrahedron.

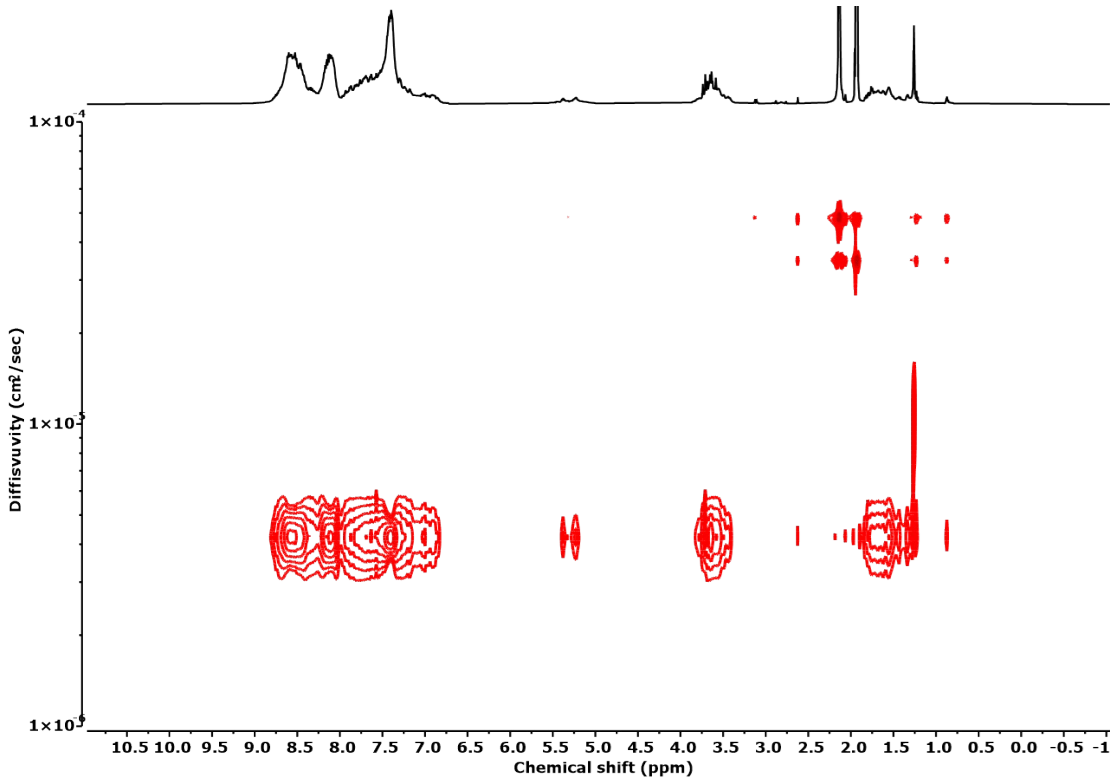

Figure S20: ^{1}H 2D DOSY NMR (500 MHz, CD_3CN, 298K) of $[Fe_4\mathbf{L}^{4}_6](PF_6)_8$ tetrahedron.

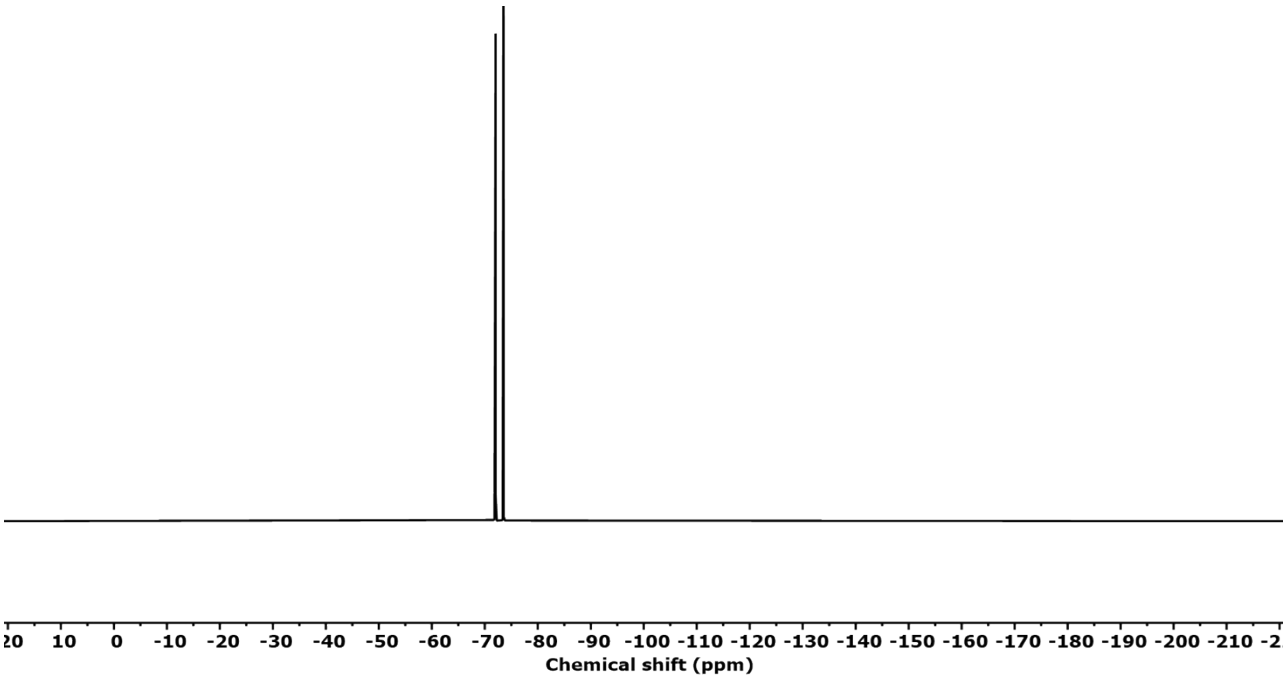

Figure S21: ^{19}F NMR spectrum (CD_3CN, 470 MHz, 298 K) for $[Fe_4\mathbf{L}^4_6](PF_6)_8$.

.

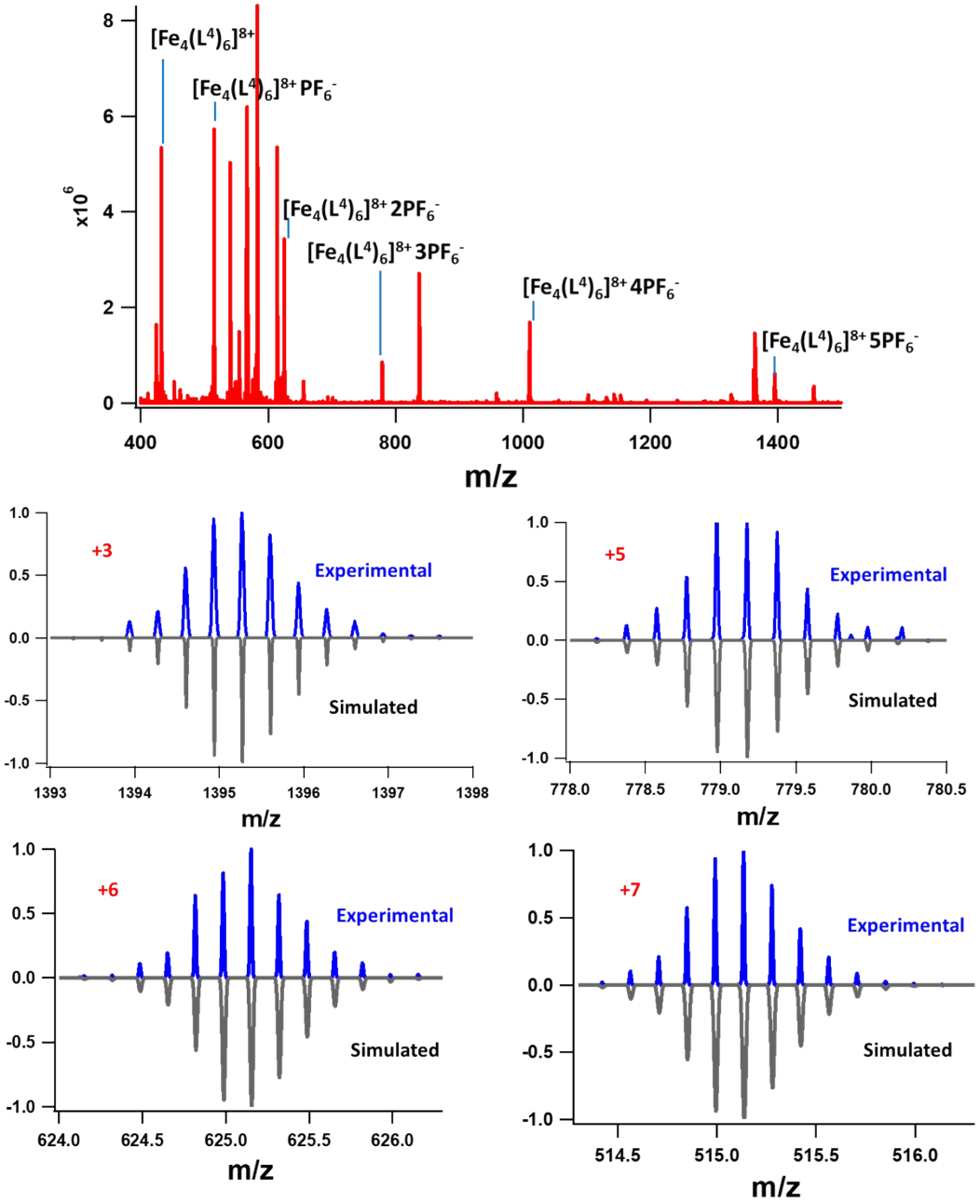

Figure S22: ESI-MS of the product +3, +4, +5, +6, +7 and +8 ions detected that correspond successive losses of PF_6^- ions from an $[Fe_4\mathbf{L}^4{}_6](PF_6)_8$.

Crystallography

Data were collected at either the MX1 beamline of the Australian synchrotron with silicon double crystal monochromated radiation (0.7108 Å) at 100(2) K or with a RigakuOD XtaLAB Synergy using micro-focused MoKα radiation. Data were indexed, reduced and integrated either XDS[3] or CrysAlisPro.[4] The solutions for diffraction data were obtained using SHELXT [5] before refinement with SHELXL[6] through the OLEX-2 GUI.[7] In order to remove the contribution of associated electron density of highly disordered solvent molecules and anions, the SQUEEZE[8] function of PLATON[9] was employed when necessary. Generally, non-hydrogen atoms with occupancies greater than 0.5 were refined anisotropically. Hydrogen atoms bound to carbon were included in idealised positions and refined using riding model. Standard crystallographic methods including constrains, restraints and rigid bodies were used to model the disorder wherever required. Specific details for each refinement are given below.

X-ray data for L^3

White needles suitable for X-ray diffraction were grown from methanol (Fig. S23). The crystals, however, were of low quality and even with Synchrotron radiation the diffraction properties of the crystal were less that ideal (broad and poor resolution) resulting in relatively high residuals. Despite these difficulties the connectivity is unambiguous. There are number of non-classical hydrogen and weak offset π- π interactions among the molecules.

$C_{76}H_{64}N_{20}O_8$ (M =1385.47 g/mol): orthorhombic, space group $P2_12_12_1$ (no. 19), a = 5.4710(11) Å, b = 12.167(2) Å, c = 50.751(10) Å, V = 3378.3(11) Å^3, Z = 2, T = 100(2) K, μ(synchrotron) = 0.093 mm^{-1}, *Dcalc* = 1.362 g/cm^3, 42922 reflections measured (3.442° ≤ 2Θ ≤ 50.248°), 6042 unique (R_{int} = 0.1433, R_{sigma} = 0.0647) which were used in all calculations. The final R_1 was 0.1236 (I > 2σ(I)) and wR_2 was 0.3588 (all data).

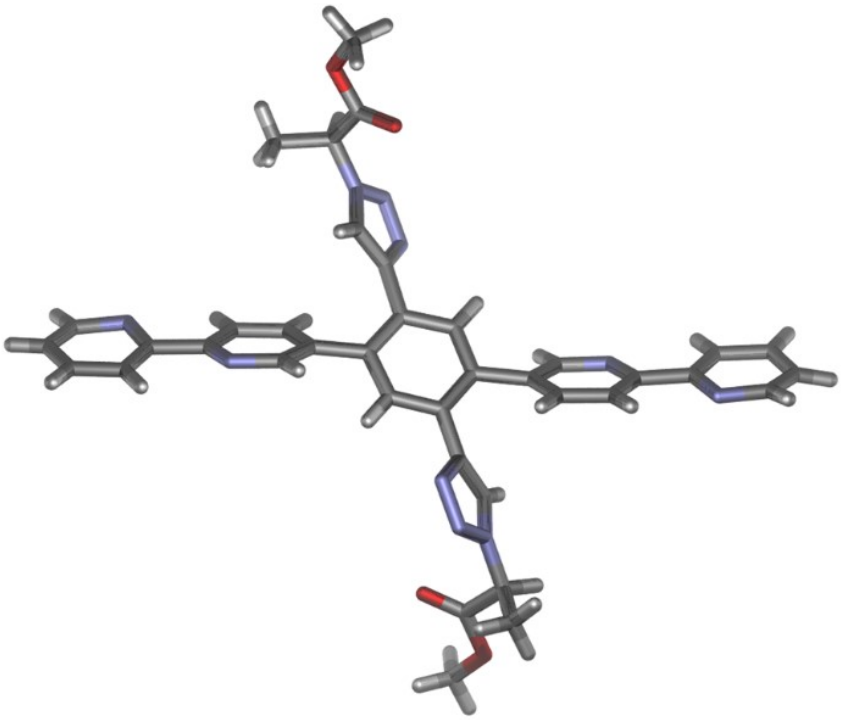

Figure S23: X-ray structure of **L^3**

X-ray data for L^4

White needles suitable for X-ray diffraction were grown from methanol by slow evaporation. **L^4** crystallised in the chiral space group *P*1 and there are two molecules in the asymmetric unit. There are number of non-classical hydrogen and week off set π- π interactions among the molecules. The crystal structure of **L^4** is shown in Fig. S24. There is some disorder present in one of the two molecules in the asymmetric unit.

$C_{32}H_{25}N_7O_2$ (M =539.59 g/mol): triclinic, space group P1 (no. 1), a = 8.32580(10) Å, b = 13.2735(2) Å, c = 13.4369(2) Å, α = 64.991(2)°, β = 86.277(2)°, γ = 73.1680(10)°, V = 1285.23(4) Å^3, Z = 2, T = 100(2) K, μ(MoKα) = 0.091 mm^{-1}, $Dcalc$ = 1.394 g/cm^3, 45708 reflections measured (3.704° ≤ 2Θ ≤ 56.564°), 12388 unique (R_{int} = 0.0350, R_{sigma} = 0.0283) which were used in all calculations. The final R_1 was 0.0439 (I > 2σ(I)) and wR_2 was 0.1234 (all data).

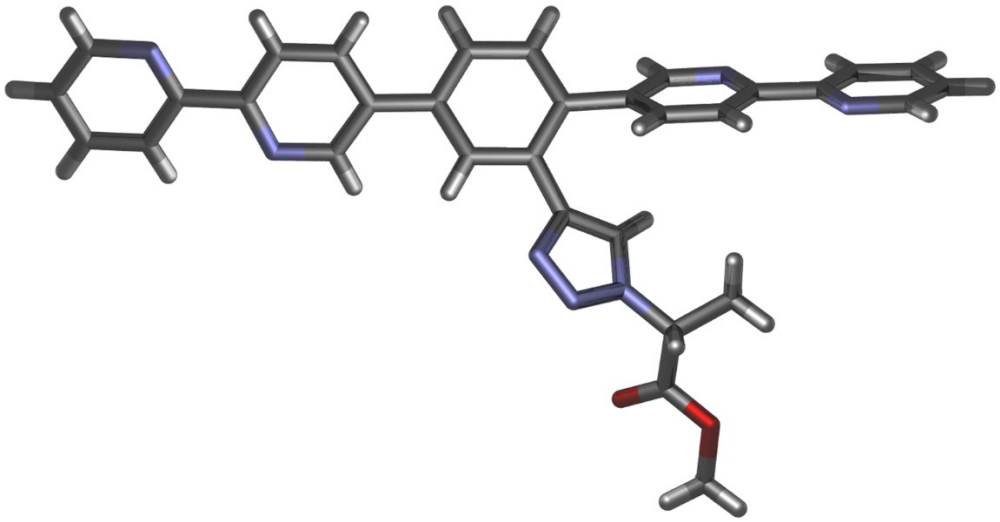

Figure S24: X-ray structure of **L^4**

X-ray data for $[Fe_2L^3_3](BF_4)_4 \cdot MeCN$

The red coloured crystals, suitable for X-ray structure determination, were grown by slow diffusion of methanol into a solution of complex in acetonitrile. The complex crystallised in space group $P2_1$ and asymmetric unit contains both diastereomers of complex that is *S,S,S,S,S,S,ΔΔ*-$[Fe_2\mathbf{L}^3_3]^{4+}$ and *S,S,S,S,S,S,ΛΛ*-$[Fe_2\mathbf{L}^3_3]^{4+}$, as shown in Fig. S25. There is some disorder in two of the side chains suggesting partial epimerisation of some of the ligand under microwave conditions. The solvent mask[10] functionality of OLEX2[11] was employed to remove the contributions from a region of smeared electron density, the number of electrons of which correspond to a BF_4^- anion, which could not otherwise be located and an acetonitrile solvent molecule.

$C_{116}H_{99}B_4F_{16}Fe_2N_{31}O_{12}$ (M =2578.20 g/mol): monoclinic, space group $P2_1$ (no. 4), a = 26.3794(6) Å, b = 14.7997(2) Å, c = 30.8356(5) Å, β = 91.093(2)°, V = 12036.2(4) Å^3, Z = 4, T = 100(2) K, μ(MoKα) = 0.340 mm^{-1}, *Dcalc* = 1.423 g/cm^3, 149906 reflections measured (4.134° ≤ 2Θ ≤ 50.7°), 43633 unique (R_{int} = 0.0904, R_{sigma} = 0.0872) which were used in all calculations. The final R_1 was 0.0792 (I > 2σ(I)) and wR_2 was 0.2206 (all data).

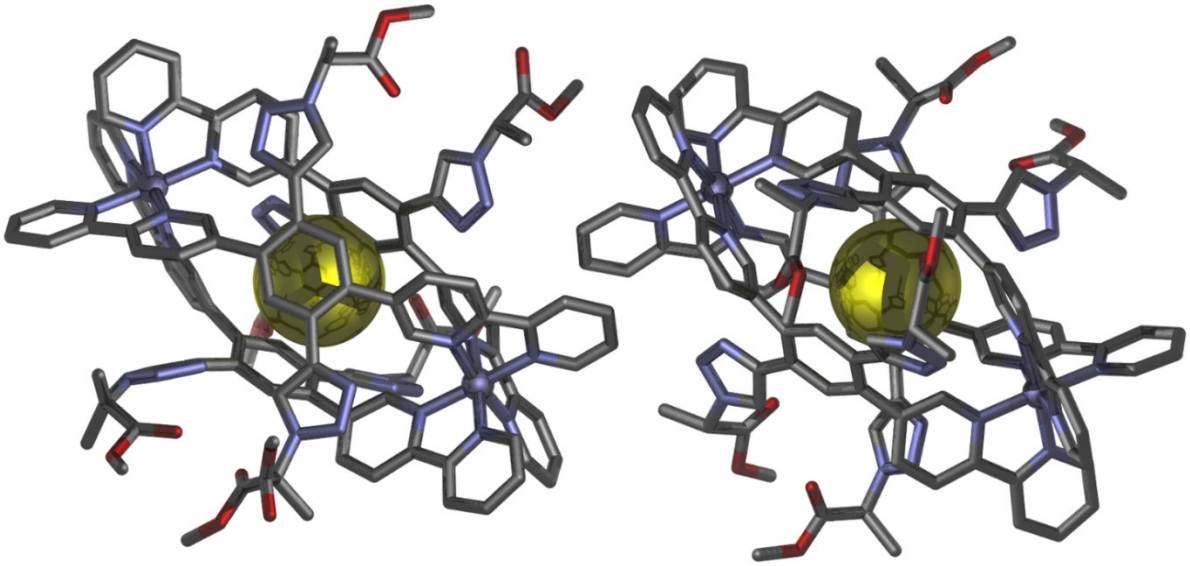

Figure S25: X-ray structure of of helical $[Fe_2\mathbf{L}^4_3]^{4+}$ assembly and yellow spheres represent the void space in the assembly.

References

1. A. Paul, H. Bittermann and P. Gmeiner, *Tetrahedron*, 2006, **62**, 8919-8927.
2. C. J. Cavender and V. J. Shiner, Jr., *The Journal of Organic Chemistry*, 1972, **37**, 3567-3569.
3. W. Kabsch, *Acta Crystallogr D Biol Crystallogr*, 2010, **66**, 125-132.
4. Rigaku OD CrysAlisPro, 2009-2021
5. G. M. Sheldrick, *Acta Crystallogr A Found Adv*, 2015, **71**, 3-8.
6. G. M. Sheldrick, *Acta crystallographica. Section A, Foundations of crystallography*, 2008, **64**, 112-122.
7. O. V. Dolomanov, L. J. Bourhis, R. J. Gildea, J. A. K. Howard and H. Puschmann, 2009, **42**, 339-341.
8. A. L. Spek, *Acta crystallographica. Section C, Structural chemistry*, 2015, **71**, 9-18.
9. A. L. Spek, *Acta Crystallogr D Biol Crystallogr*, 2009, **65**, 148-155.
10. P. van der Sluis and A. L. Spek, *Acta Cryst.*, 1990, **46**, 194-201.
11. O. V. Dolomanov, L. J. Bourhis, R. J. Gildea, J. A. K. Howard and H. Puschmann, *J. Appl. Cryst.*, 2009, **42**, 339-341.